Published Online First: August, 2024
https://doi.org/10.21123/bsj.2024.9373
P-ISSN: 2078-8665 - E-ISSN: 2411-7986
Baghdad Science Journal

Green Innovation in Environmental Remediation: J10-PET Thin Films for Efficient Removal of Methylene Blue and Methyl Orange Contaminants

Jihan A. Mustafa [1] ***,Parween H. Saleem*** *[1] ***, Huda A. Basheer*** [2]

[1]Department of Chemistry, College of Science, University of Duhok, Duhok, Iraq.
[2]Department of Chemistry, Faculty of Science, University of Zakho, Duhok, Iraq.
*Corresponding Author.

Received 11/09/2023, Revised 28/11/2023, Accepted 30/11/2023, Published Online First 20/08/2024

Abstract

This study introduces an innovative approach employing N-(3-benzylureido)(methyl)-2-(6-methoxynaphthalen-2-yl)propanamide (J10) as an additive for recycled polyethylene terephthalate (PET) to produce thin film (J10-PET thin film), with a focus on their application in the removal of methylene blue (MB) and methyl orange (MO) from aqueous solutions. The study is primarily focused on unraveling the kinetics and equilibrium behaviors governing the removal of MB and MO. The investigation includes the determination of the equilibrium adsorption capacities (Q_e) of MB and MO at different temperatures (308, 323, and 333 K) and concentrations (5, 10, and 15 mg/g). Remarkably, the pseudo-second-order model is found to best elucidate the adsorption kinetics for both MB and MO. Notably, the J10-PET thin film exhibits promising results with an activation energy of 14.42 kJ/mol for MB and 36.08 kJ/mol for MO, indicating its potential for effective pollutant removal. This research contributes to a comprehensive understanding of adsorption processes and highlights the J10-PET thin film as a promising solution for addressing MB and MO pollutants in aqueous environments.

Keywords: Adsorption, Expired pharmaceuticals, Kinetics, Methylene blue (MB), Methyl orange (MO), PET solid waste, Thin film, Wastewater treatment.

Introduction

Water contamination is a pressing global issue exacerbated by industrialization and population growth, driven by the increasing quantity of wastewater released into water systems[1]. Synthetic dyes, extensively used in industries such as textiles, food, printing, and pharmaceuticals, are among the leading contributors to water pollution[2] .

Dyes are organic chemicals used in various industries, including textiles, paper, food, printing, plastics, beverages, leather, and pharmaceuticals[3,4]. Approximately 0.8 million tonnes of organic dyes, including over 10,000 different types, are produced annually [5], with alarming statistics indicating that approximately 15% of these dyes are lost during various processing activities, releasing toxic organic substances into water systems[2,6,7]. A significant portion of these dyes consists of anionic (acidic) and cationic (basic) dyes [8] , with azo dyes, containing nitrogen-nitrogen double bonds[9], being the most comprehensive [10], and a major environmental concern due to their carcinogenic metabolites. [11–13]

MB is a common type of cationic thiazine dye used for dying wood, cotton, silk, and leather; also used in medicine, as an antiseptic, and in the sciences

Published Online First: August, 2024
https://doi.org/10.21123/bsj.2024.9373
P-ISSN: 2078-8665 - E-ISSN: 2411-7986
Baghdad Science Journal

(chemistry, biology) laboratories[14]. Because MB is so poisonous, its presence in water can do much damage to the human body, producing conditions such as nausea, anemia, dizziness, jaundice, and chest pain[15], Long-lasting harm to the eyes and skin can occur, along with the possibility of causing negative impacts on living organisms. These can manifest as symptoms like confusion, profuse sweating when inhaled through water, digestive issues such as diarrhea[16], and vomiting, as well as discomfort in the mouth, throat, and stomach leading to feelings of nausea.[8, 17]

Similarly, MO an azo dye that can dissolve in water, is often found in the wastewater discharged by various industries such as textiles, food processing, pharmaceuticals, printing, and paper manufacturing,[18,19] this dye is among the most commonly encountered pollutants in water systems due to the toxicity and persistence the discharges can cause severe threats to the physicochemical properties of fresh water and aquatic life. Thus, removing MB and MO from aqueous solutions is essential [20]. Removing MO from wastewater poses challenges due to its complex aromatic ring structure, resistance to degradation, xenobiotic properties, high visibility under strong light, stability, and resistance to oxidation.[21]

In recent years, researchers have dedicated significant efforts to test and advance various techniques for eliminating dyes from wastewater. These methods include coagulation, chemical oxidation, biodegradation, ultrasonic degradation, photodegradation, membrane separation, and adsorption.[1, 22]

However, many of these methods come with drawbacks, such as high costs and the generation of secondary waste products. Among these techniques, adsorption stands out as the most suitable method[23] due to its cost-effectiveness, flexibility, and ability to efficiently remove a wide range of pollutants without producing hazardous chemicals.[24,25]

Plastic items have become vital to our daily lives in recent decades. PET is the most widely used polymer in food, medicine, and soft drink bottle and container manufacturing due to its lightweight, low cost, transparency, sound insulation, Outstanding tensile properties, resistance to chemicals, ease of use, and flexibility;[26,27] Consequently, there has been a notable rise in the generation of PET solid waste every year, resulting in significant ecological concerns[28] . Due to its non-biodegradability, inappropriate mechanical qualities, thermal stability, and reduced electrical conductivity, PET is the most abundant municipal and industrial waste but has no beneficial purpose[29]. Thus, PET waste disposal is a global issue, especially in developing nations. Incineration and landfilling are prominent PET waste management methods [30] ; however, these technologies may harm the environment by emitting heat, volatile chemicals, and landfill contamination. The chemical recycling of PET has many processes. The main obstacles to PET chemical recycling are scale-up, cost, and organic solvent handling.[31]

Many researchers are interested in developing creative, affordable, and ecologically acceptable adsorbent compounds from PET bottle waste, including activated carbon,[32,33] Recycled PET, Fibres Modified with Graphene Oxide[34] modified (phenol-PET)[35] and PET Nanofibrous membranes[36] for the removal of pollutants from wastewater.

The increase in the production and consumption of drugs has led to an exponential rise in the improper disposal of drugs.[37,38] Expiring medications are complicated chemicals that can pollute water, soil, and animals. Additionally, outdated drugs may be hazardous or ineffective [39].

Based on a study by Chinese researchers, 20 tonnes of expired pharmaceuticals and 724.5 tonnes of disinfection products were destroyed. Drug expiration impacts health issues and hurts the government due to the loss of funds allotted for the health sector. In a study conducted in Africa, particularly in East Africa, the amount of money lost due to expired medications was unexpected.[40]

Recent studies investigated ways to recycle active pharmaceutical ingredients (API) from pharmaceuticals. For instance, Pratama et al. used solid-liquid extraction to recover API from expired paracetamol, tetracycline, and ibuprofen. The study found that the optimal solvent composition can retain highly pure API with recovery yields of 58.7%, 73.1%, and 67.6% for paracetamol, tetracycline, and ibuprofen when removing the most excipients[41]

The objective of this study is to investigate the adsorption capabilities of MB and MO on J10- PET thin film. The J10 compound was synthesized using expired naproxen drug and PET from discarded water bottles. The thin film was created by mixing and dissolving a mixture of compound J10 with PET

Published Online First: August, 2024
https://doi.org/10.21123/bsj.2024.9373
P-ISSN: 2078-8665 - E-ISSN: 2411-7986
Baghdad Science Journal

and casting it into the desired thin film shapes that were used as an effective adsorbent to remove methyl blue and methyl orange from wastewater.

Materials and Methods

Chemicals

N-(isocyanatomethyl)-2-(6-methoxynaphthalen-2-yl)propanamide;Bilim Pharmaceutical; benzylamine from(Sigma-Aldrich); Toluene from (Uni-Chem); diethyl ether from (Biosolve B.V); The polymer (PET) waste material is sourced from a (local water packaging company), initially undergoing washing and removal of non-PET components, followed by a drying process. All chemicals utilized in the study are of high-quality analytical reagent grade. Trifluoroacetic acid (TFA) is acquired from (ROTH), dichloromethane (DCM) from (Uni-Chem), while methyl orange (MO) and methylene blue (MB) are obtained from (Sigma-Aldrich). sodium hydroxide (NaOH) and hydrochloric acid (HCl) were obtained from Scharlau, ensuring the use of high-purity chemicals from a reputable supplier for all experimental procedures.

Experimental

Preparation and characterization of N-((3-benzylureido)methyl)-2-(6-methoxynaphthalen-2-yl)prpopanamide (J10)

A mixture containing N-(isocyanatomethyl)-2-(6-methoxynaphthalen-2-yl) propanamide (2.84g, 0.01mole) and benzylamine (1.07g, 0.01mole) was exposed to reflux in dry toluene (25 ml) for 72 hours on a sand bath. After the reflux period, the surplus toluene solvent was eliminated under reduced pressure, yielding a residue, and diethyl ether was used to wash the residue. The resulting solid product was subjected to a recrystallization procedure. The recrystallization was executed using a solvent mixture composed of ethanol and water. Fig. 1 shows the structure of J10.

Yield: 91%, mp: 98-100 C0; brown solid; eluent:(hexane: ethyl acetate 1:1) Rf =0.21; 1H NMR (CHCl3-d) δ (ppm): 1.50-1.56 (d, J=8 Hz ,3H) CHCH3; 3.66-3.75 (q, J=8 Hz, 1H) CHCH3; 3.85 (s,2H) NHCH2Ar; 3.90(s,3H) OCH3; 4.30(s,2H) NHCH2NH; 7.09 -7.83(m,11H) Ar-H ;6.60,6.89, 8.40 (b,3H) 3NH; 13C-NMR (CHCl3-d) δ (ppm): 18.27 CHCH3;43.36 CHCH3; 46.61 NHCH2NH ; 55.30 OCH3; 66.04NHCH2Ar; 105.58, 119.19, 125.93, 126.99, 127.43, 127.57, 127.97, 128.60, 128.90, 129.22, 133.74, 137.75, 139.21, 157.70 (16C) Ar-C; 168.81, 175.11(2C=O); IR (KBr), ν (cm^{-1}): 3306, 3200, 1630, 1605, 1264.

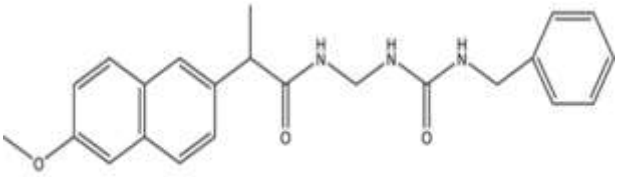

Figure 1. Structure of N-(3-benzylureido) methyl)-2-(6 methoxynaphthalen-2-yl) propanamide (J10)

Preparation of polymer Solution

A PET polymer solution is created by dissolving 0.28g of PET and 0.06g of J10 in a solvent mixture composed of DCM and TFA (in a ratio of 3:1). Initially, PET is ground using a common household grinder and then sifted through a test sieve (with a mesh size of 250 μm). The PET solution is stirred using a magnetic stirrer at room temperature for the duration of four hours to enhance the polyethylene's solubility[42].

Preparation of J10- PET thin film

The polymer solution is transformed into a thin film through a casting process. The prepared polymer solution is initially spread onto a substrate, forming a layer. The solvent is subsequently eliminated through evaporation, forming a solid film adhering to the substrate. This cast layer is then separated from the substrate, yielding an independent thin film. This procedure successfully produces a thin film with a thickness ranging from 27 to 36 micrometers. To facilitate subsequent utilization, the thin film is divided into pieces weighing 0.01 grams.

The morphologies between the PET thin film and the J10-PET thin film are compared using a field emission scanning electron microscope (TESCAN), Fourier transforms infrared spectra (FTIR) (Shimadzu), and the measurements of the thermal gravimetric analysis (DSC-TGA) are attested with (Q600).

Preparation of Solutions

Published Online First: August, 2024
https://doi.org/10.21123/bsj.2024.9373
P-ISSN: 2078-8665 - E-ISSN: 2411-7986
Baghdad Science Journal

To prepare the MB and MO stock solutions at a concentration of 1000 mg/L, 0.01 g of MB and MO were individually dissolved in 100 ml of deionized water, resulting in 100 mg/L stock solutions. Workable solutions with concentrations of 3, 5, 7, 9, 11, and 13 mg/L for both MB and MO were obtained by dilution with water.

For the creation of a 0.1 mol/L HCl stock solution, 2.1 ml of concentrated HCl (12.07 mol/L) was diluted with 250 ml of distilled water, yielding the desired concentration. Working solutions were subsequently prepared through further dilutions with water.
In a 250 ml volumetric flask, a 0.4 g quantity of NaOH was dissolved in distilled water to produce a stock solution with a concentration of 1.0 mol/L NaOH.

Batch Adsorption Studies of MB and MO

The adsorption of MB and MO is conducted in a batch process by employing different doses of J10-PET thin film adsorptive, variable concentrations of MB and MO, and adjusting the pH and temperature.

A measured quantity of the dehydrated J10-PET thin film is combined with a 10 ml solution of either MB or MO, with concentrations that vary. The solution is agitated in a temperature-controlled water bath for 30 minutes. The concentrations of MB and MO are determined using a spectrophotometer of the Janeway 7315 type after the adsorption process. These concentrations are obtained by referencing a calibration curve with a contrast measurement.

Impact of Contact Time and Temperature on Adsorption

The influence of temperature on the adsorption process of MB and MO onto the J10-PET thin film was explored. This was achieved by mixing 5 ml of MB or MO solution (with concentrations of 5 mg/L at pH 12 for MB and pH 3 for MO) with 0.01g of the J10-PET thin film. The experiments were conducted at various temperatures (308, 323, and 333 K) while agitating the mixture at 150 rpm for varying durations (ranging from 5 to 140 minutes).

Impact of Contact Time and (MB and MO) Concentrations on Adsorption

The impact of initial concentration on the adsorption of MB and MO onto the J10-PET thin film was assessed. This involved combining 5 ml of solutions with different initial MB or MO concentrations (5, 10, and 15 mg/L) at pH 12 for MB and pH 3 for MO, with 0.01 g of the J10-PET thin film. The experiments were carried out at a temperature of 308 K, while agitating the mixture at 150 rpm for durations ranging from 5 to 140 minutes.

Investigation of Adsorption Kinetics

Analyzing changes in adsorption capacity over time offers valuable insights into adsorption kinetics. It is crucial to comprehend the specific adsorption mechanism in a given system. To characterize the kinetics of MB and MO adsorption onto the J10-PET thin film, four kinetic models were employed: pseudo-first-order, pseudo-second-order, Elovich, and intraparticle diffusion. These models aid in shedding light on the adsorption process behavior as it unfolds over time. [43, 44]

Results and Discussion

Fig. 2 depicts scanning electron microscopy (SEM) images showcasing the morphological features of both the PET thin film and the J10-PET thin film. In Fig. 2A, the PET thin film exhibits a uniform and smooth surface. In contrast, Fig. 2B illustrates the J10-PET thin film, which displays agglomerates comprising grains of varying sizes. This data compellingly demonstrates the interaction between the J10 chemical and the PET particles, leading to the noticeable formation of particle clusters.

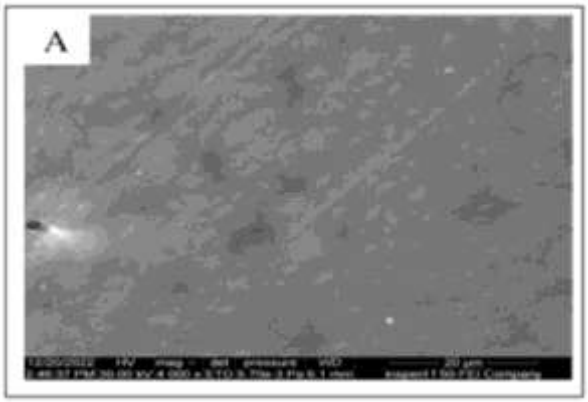

Published Online First: August, 2024
https://doi.org/10.21123/bsj.2024.9373
P-ISSN: 2078-8665 - E-ISSN: 2411-7986
Baghdad Science Journal

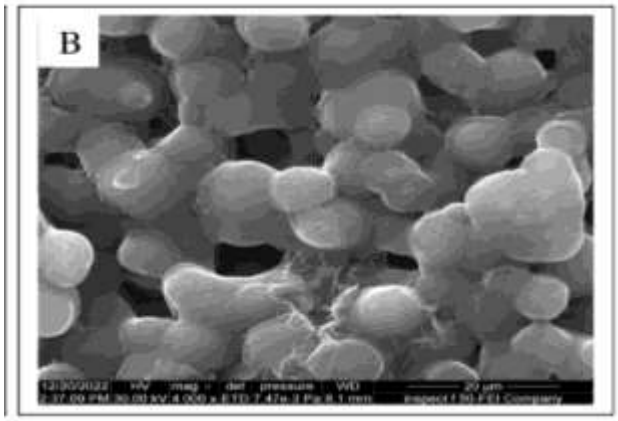

Figure 2. SEM Micrographs of A) PET thin film B) J10- PET thin film

The specific peaks detected in the FTIR spectra, including those in the amide range typically spanning 1600-1800 cm^{-1} and 1250-1350 cm^{-1}, are indicative of characteristic infrared signatures associated with the J10 compound. Additionally, the presence of peaks at 1836, 1797, and 1708 cm^{-1} aligns with carbonyl (C=O) stretching vibrations, a well-recognized feature of amides. The absorption band at 1678 cm^{-1}, which corresponds to C=O stretching vibrations, further substantiates the presence of amide groups within the J10 compound. The bands at 1242 and 1199 cm^{-1} are in agreement with C-N stretching vibrations, consistent with the chemical structure of the J10 compound. Furthermore, the absorption band at 717 cm^{-1}, attributed to out-of-plane bending vibrations of aromatic C-H bonds, aligns with the anticipated characteristics of aromatic compounds found in the J10 compound Fig. 3A. These FTIR results provide strong confidence in the presence and characteristics of the J10 compound on the surface of the thin film.

The presence of active functional groups on the surface of the J10-PET thin film serves as a crucial factor in its role as an adsorbent for MB and MO. To discern any changes in the positions of these active functional groups after MB and MO adsorption, FTIR spectra of the J10-PET thin film post-adsorption were collected using an FTIR spectrometer Fig. 3B, 3C.

Notably, the redshift observed in the peaks at positions 1678 and 1242 cm-1for MO and MB after adsorption provides compelling evidence of the interaction between the adsorbent and the adsorbate, further elucidating the adsorption mechanism.[45, 46]

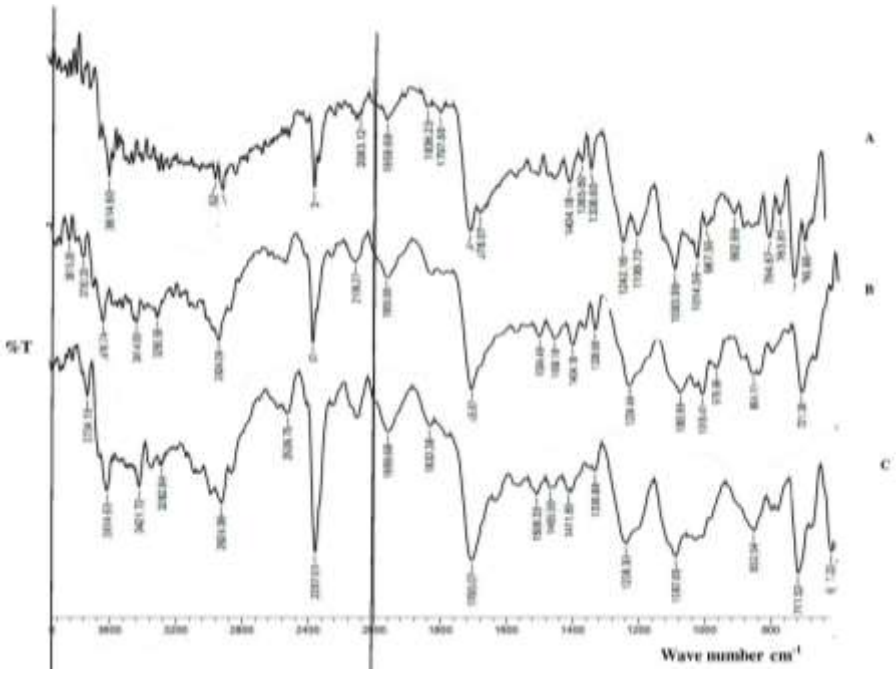

Figure 3. FTIR Spectra of A) J10- PET thin film B) J10- PET thin film after adsorption of MO C) J10- PET thin film after adsorption of MB

Impact of Contact Time and Temperature on Adsorption

Fig. 4A, B depict plots showing the adsorbed quantities of MB and MO, denoted as Q_e (mg/g), about the contact time at different temperatures (308, 323, and 333 K). Notably, there is a conspicuous trend wherein the uptake of both MB and MO, represented by Q_t (mg/g), exhibits a rapid surge

Published Online First: August, 2024
https://doi.org/10.21123/bsj.2024.9373
P-ISSN: 2078-8665 - E-ISSN: 2411-7986
Baghdad Science Journal

within the initial 10 minutes across all temperature levels, indicative of film diffusion, where the adsorbate molecules on the surface of the adsorbent quickly establish a thin layer, or film," due to the high concentration gradient between the bulk solution and the surface. A swift adsorption rate characterizes this process during the early stages of contact. Beyond this period, the rise in adsorbed quantities becomes more gradual, suggesting the involvement of pore diffusion, eventually culminating in equilibrium around the 100-minute mark.[47]

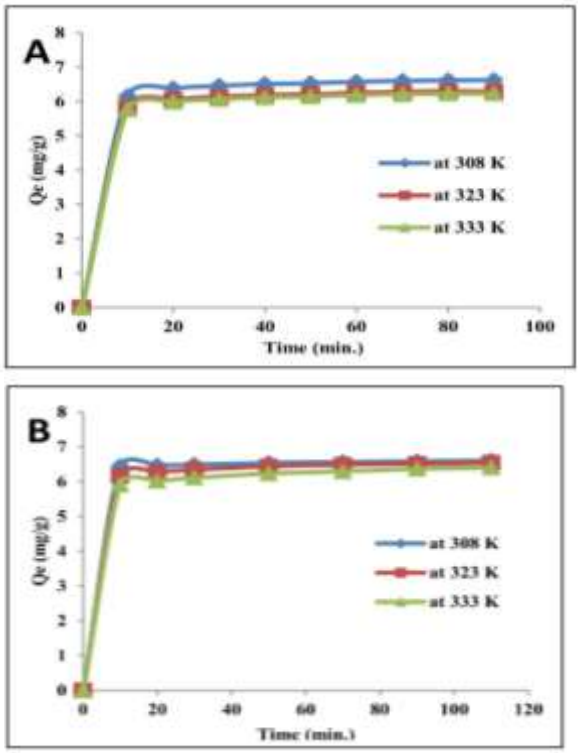

Figure 4. Impact of contact time and temperature on the adsorption of A) MB B)MO on J10- PET thin film

Impact of Contact Time and Dyes Concentration on Adsorption

The initial concentrations of both MB and MO are crucial factors in facilitating the effective transfer of these molecules between the aqueous and solid phases, especially when dealing with potential resistance. The adsorption behavior of MB and MO onto the J10-PET thin film was examined in relation to contact time and varying initial concentrations, as shown in Figs. 5A, B. The results revealed a common trend across all concentrations. Initially, during the first ten minutes of contact, the adsorption process was rapid, and it progressively increased as the contact time extended until it reached equilibrium. Furthermore, it was observed that increasing the initial concentrations of MB and MO led to a corresponding increase in Q_t within the initial ten minutes. This behavior can be attributed to the higher initial concentrations creating greater momentum within the pores, thereby enhancing the adsorption capacity[48]. These findings closely parallel previous research on the adsorption of methylene blue dye using a carbonaceous hydro char adsorbent.[49]

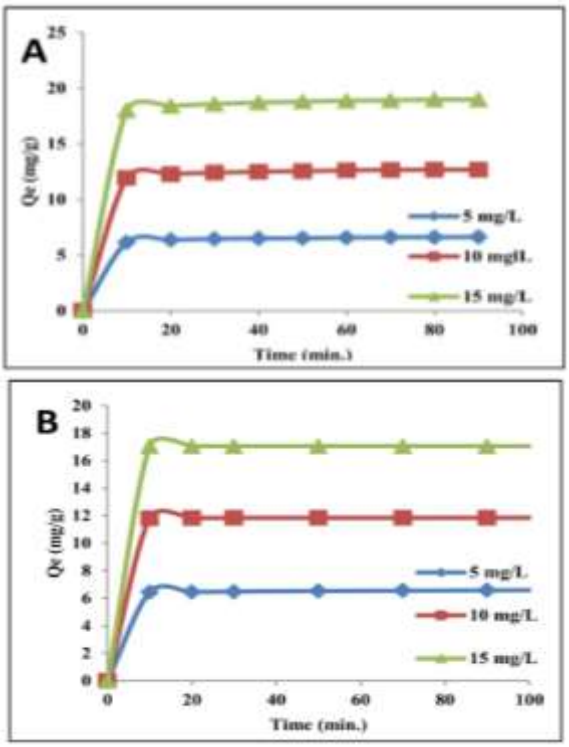

Figure 5. Impact of contact time and MB concentration on the adsorption of A) MB B) MO on J10- PET thin film

Investigation of Adsorption Kinetics

Estimating sorption mechanisms and rate-control processes is crucial in determining the optimal operating parameters for the complete batch process. To do this, four kinetic models are employed. The adsorption capability of MB and MO onto a thin film of J10-PET is seen at various concentrations and temperatures. The monitoring is done over time until a steady state is achieved, indicating a constant amount of MB and MO adsorbed. The adsorption process entails the attainment of balance. The equilibrium time is constant at 100 minutes across all concentrations and temperatures examined. The Q_e of MB and MO onto J10-PET thin film is directly related to the initial concentrations of MB and MO and the temperatures at which the adsorption process

Published Online First: August, 2024
https://doi.org/10.21123/bsj.2024.9373
P-ISSN: 2078-8665 - E-ISSN: 2411-7986
Baghdad Science Journal

happens. The tables provided in this study reflect the equilibrium adsorption capacity values achieved across various experimental settings, as outlined in Tables 1,2.

Impact of Temperature on Adsorption Kinetics

The impact of temperature on the pseudo-first order adsorption kinetics of MB and MO onto a J10-PET thin film is illustrated in Figs. 6A, B.

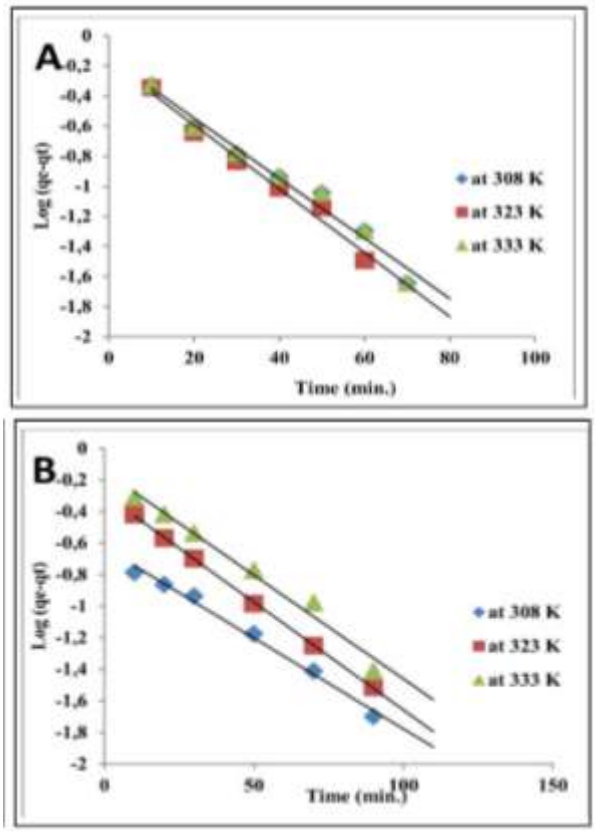

Figure 6. Pseudo-first order adsorption kinetics of the adsorption of A) MB B) MO on J10- PET thin film

Even though the experimental data gave correlation coefficients ($R^{2)}$ that were quite large, exceeding 0.958, it is clear from Table .1 that the calculated equilibrium sorption capacities Q_t do not match the experimental values. This finding suggests the pseudo-first-order model is unsuitable for accurately predicting MB and MO's adsorption behavior onto a J10-PET thin film.

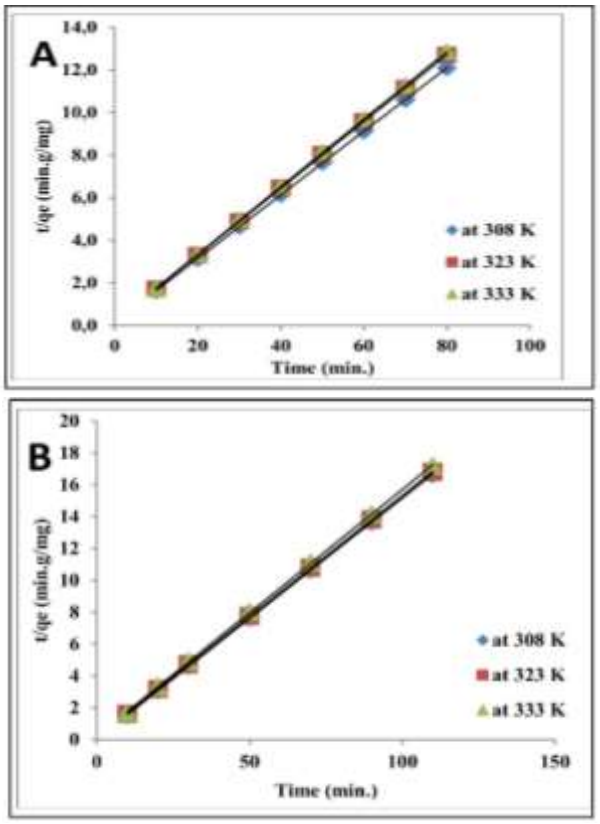

Figure 7. Pseudo-second order adsorption kinetics of the adsorption of A) MB B) MO on J10- PET thin film

Fig. 7 depicts the kinetics of pseudo-second-order adsorption for MB and MO dyes on a J10-PET thin film under varying temperature conditions (308, 323, and 333 K). The figure illustrates the relationship between time and the degree of adsorption for both dyes. A notable finding is the consistent linear correlation observed across varying temperature conditions. This strong linear relationship indicates the suitability of the pseudo-second-order kinetic model for describing the adsorption process.

The Elovich equation is a rate equation that is derived from the consideration of adsorption capacity. Fig. 8 displays a plot of qt against ln (t). If the adsorption of MB and MO on the J10-PET thin film is consistent with the Elovich model, then a plot of q_t versus ln (t) reveals a linear relationship with high R^2.

Published Online First: August, 2024
https://doi.org/10.21123/bsj.2024.9373
P-ISSN: 2078-8665 - E-ISSN: 2411-7986
Baghdad Science Journal

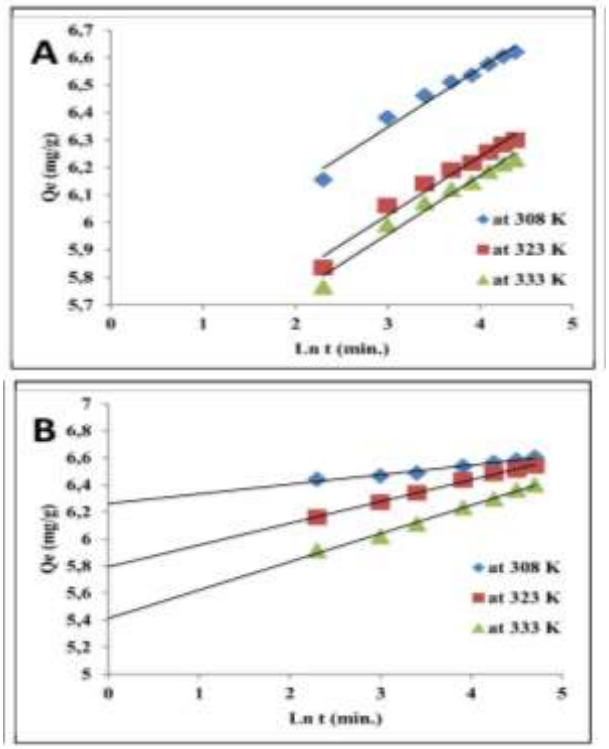

Figure 8. Elovich kinetic for adsorption kinetics of the adsorption of A) MB B) MO on J10- PET thin film

Intraparticle diffusion kinetics is a concept used to describe the rate at which solute molecules or ions diffuse into the interior of solid adsorbent material during an adsorption process. The intraparticle diffusion model is often used to describe the diffusion-controlled step of the adsorption process. The model assumes that the adsorption rate is influenced by the diffusion rate of the solute within the adsorbent particles. Fig. 9 illustrates the impact of temperature on the intraparticle diffusion kinetics of MB and MO.

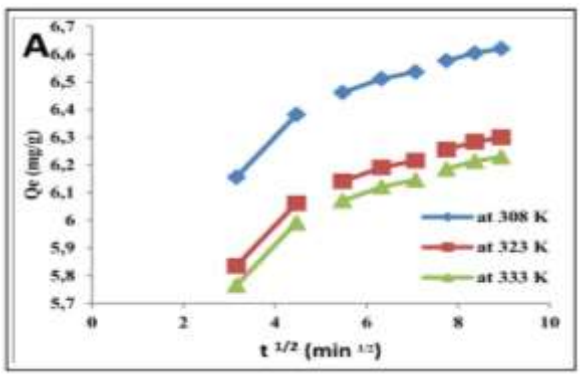

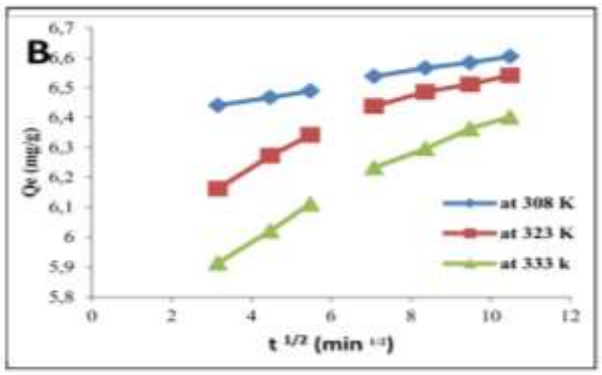

Figure 9. Intraparticle diffusion for adsorption kinetics of the adsorption of A) MB B) MO on J10- PET thin film

Impact of Initial Dyes Concentration on Adsorption Kinetics

Fig. 10 illustrates the pseudo-first-order sorption kinetics observed during the adsorption process of MB and MO onto the J10-PET thin film. The experiment was conducted at a temperature of 308 K, with initial dye concentrations of 5, 10, and 15 mg/L. The pseudo-first-order model exhibits an increase in the rate of constant values as the initial concentrations of the dye gradually grow.

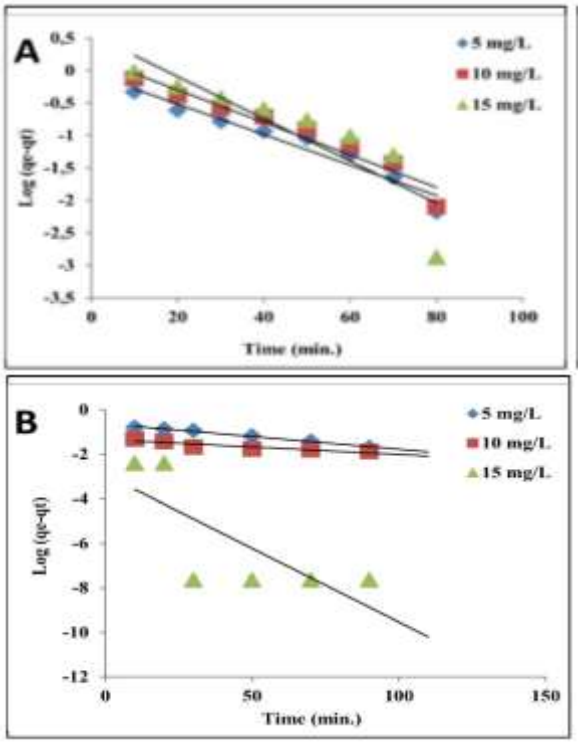

Figure 10. Pseudo-first order adsorption kinetics of the adsorption of A) MB B) MO on J10- PET thin film.

Published Online First: August, 2024
https://doi.org/10.21123/bsj.2024.9373
P-ISSN: 2078-8665 - E-ISSN: 2411-7986
Baghdad Science Journal

Fig. 11 illustrates the kinetics of pseudo-second-order adsorption for the dyes MB and MO onto a J10-PET thin film. The initial dye concentrations used in the experiment were 5, 10, and 15 mg/L, and the temperature was maintained at 308 K. A linear relationship was seen for all initial dye concentrations, with R^2 values exceeding those of pseudo first-order kinetics.

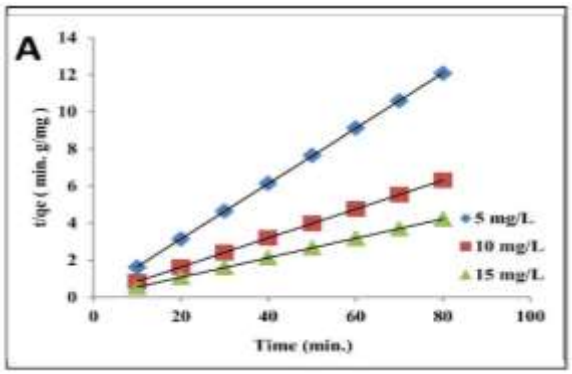

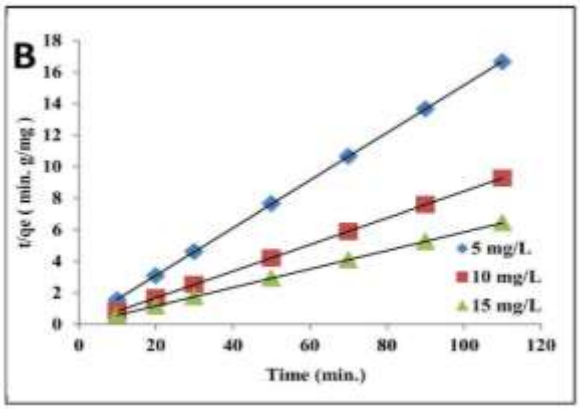

Figure 11. Pseudo-second order adsorption kinetics of the adsorption of A) MB B) MO on J10- PET thin film.

Table .1 Pseudo-first-order and Pseudo -second-order kinetic parameters of adsorption of MB and MO onto a J10-PET thin film at different temperatures and different initial MB and MO concentrations.

Dye	Temp./Conc.	Q_e (exp.)	Pseudo – first order reaction			Pseudo – second - order reaction			
			R^2	K_1	Q_e(calc.)	R^2	h	K_2	Qe(calc.)
MB	308 K	6.619	0.974	0.0458	1.414	1	10	0.225	6.666
	323 K	6.299	0.981	0.0488	1.478	0.999	8	0.194	6.410
	333 K	6.229	0.974	0.0458	1.414	0.999	5.714	0.144	6.289
	5 mg/L	6.619	0.944	0.0541	1.104	1	6.6	0.15	6.69
	10 mg/L	12.666	0.942	0.0575	1.059	1	14.7	0.09	12.79
	15 mg/L	18.965	0.781	0.0748	3.62	1	24.3	0.07	19.12
MO	308 K	6.604	0.991	0.0264	4.246	1	13.071	0.298	6.622
	323 K	6.542	0.999	0.0315	1.957	1	6.622	0.152	6.587
	333 K	6.402	0.979	0.0301	1.401	0.999	4.334	0.103	6.464
	5 mg/L	6.604	0.991	0.0265	4.25	1	13.1	0.298	6.623
	10 mg/L	11.862	0.834	0.0154	21.59	1	181.8	1.292	11.862
	15 mg/L	17.059	0.565	0.152	819.22	1	5000.0	17.170	17.065

The values representing the Elovich adsorption kinetics and rates of intra-particle diffusion can be determined by analyzing the slopes and intercepts of the plots depicted in Figs. 12,13.

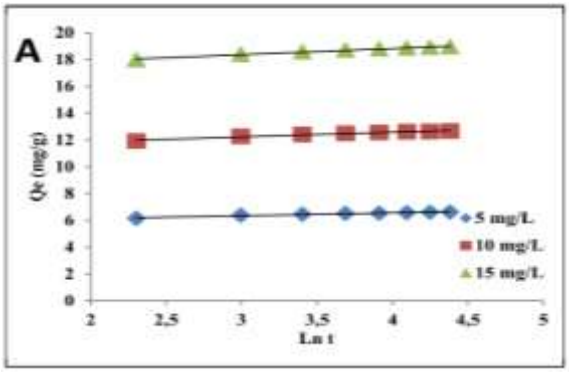

Published Online First: August, 2024
https://doi.org/10.21123/bsj.2024.9373
P-ISSN: 2078-8665 - E-ISSN: 2411-7986
Baghdad Science Journal

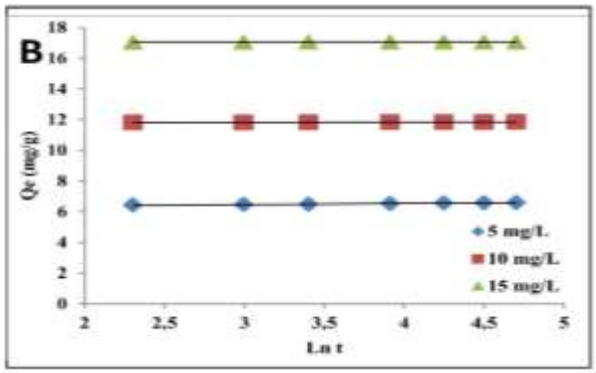

Figure 12. Elovich adsorption kinetics of the adsorption of A) MB B) MO on J10- PET thin film.

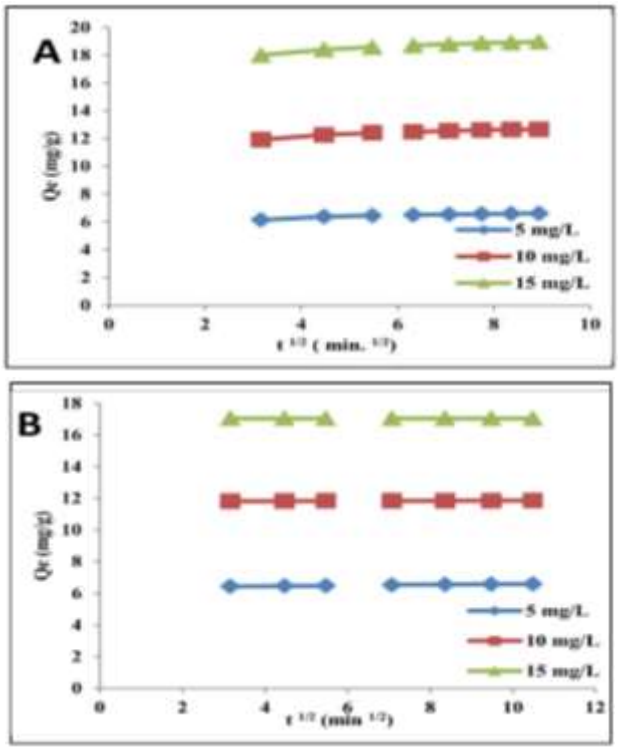

Figure 13. Intraparticle diffusion adsorption kinetics of the adsorption of A) MB B) MO on J10- PET thin film.

Table 2 Elovich and Intraparticle diffusion adsorption kinetics parameters of adsorption of MB and MO onto a J10-PET thin film at different temperatures and different initial MB and MO concentrations.

Dye	Temp./Conc.	Elovich kinetic equation			Intraparticle diffusion		
		R^2	α	β	R_2	K_{dif}	B_L
MB	308 K	0.971	25.113	4.672	0.904	0.0731	6.0095
	323 K	0.971	23.618	4.672	0.904	0.0731	5.6895
	333 K	0.971	23.291	4.672	0.904	0.0731	5.6195
	5 mg/L	0.97	25.11	4.67	0.90	0.07	6.01
	10 mg/L	0.98	30.70	2.84	0.91	0.12	11.67
	15 mg/L	0.99	36.32	2.18	0.94	0.16	17.64
MO	308 K	0.9745	85.436	14.0647	0.993	0.0231	6.3671
	323 K	0.9965	34.210	6.218	0.956	0.0507	6.0421
	333 K	0.9947	24.283	4.775	0.985	0.0671	5.7267
	5 mg/L	0.975	85.44	14.06	0.99	0.02	6.37
	10 mg/L	0.928	635.79	54.35	0.89	0.01	11.80
	15 mg/L	0.714	8967.94	526.32	0.62	0.00	17.06

The kinetics of MB and MO adsorption onto J10-PET thin film are assessed using four kinetic models: pseudo-first-order, pseudo-second-order, Elovich, and intraparticle diffusion. A higher correlation coefficient signifies a firmer fit, with a value of 1 denoting a perfect fit. The results presented in Table .1 reveal that correlation coefficients ranging from 0.999 to 1 across various temperatures (308, 323, and 333 K) and various concentrations (5, 10, and 15 mg/L indicate an exceptionally robust positive correlation between experimental data and predictions from the pseudo-second-order kinetic model.[50]

The calculated equilibrium sorption capacities, Q_e and Q_o, align closely with experimental findings. This agreement underscores the model's effectiveness in accurately representing the data,

Published Online First: August, 2024
https://doi.org/10.21123/bsj.2024.9373
P-ISSN: 2078-8665 - E-ISSN: 2411-7986
Baghdad Science Journal

suggesting a strong resemblance between observed and predicted adsorption behaviors.[49]

Consequently, the pseudo-second-order kinetic model emerges as a fitting portrayal of the adsorption process of MB and MO onto J10-PET thin film.

The findings suggest that the observed pseudo-second-order kinetics can be attributed to chemisorption, wherein the MB and MO dyes form chemical bonds with the J10-PET thin film. The pseudo-second-order kinetics model indicates that the adsorption process is predominantly governed by the interaction between the solute and the active sites of the adsorbent, resulting in the establishment of chemical bonds.[51]

As shown in Table.2, the Elovich equation of MB and MO adsorption onto J10-PET thin film also has a respectable R^2 (0.971-0.99) across various temperatures (308, 323, and 333 K) and various concentrations (5, 10, and 15 mg/L) suggesting a good fit indicates a strong positive correlation between the experimental data and the predictions made by the Elovich equation. However, this correlation is slightly weaker compared to the pseudo-second-order model. While the Elovich equation provides a good fit for data, it might not capture the data's behavior as closely as the pseudo-second-order model.

The rates of intra-particle diffusion can be estimated by analyzing the slopes of the plots illustrating qt against $t^{1/2}$, as depicted in Figs. 9,13. The linear trends observed in both figures emphasize the significant role of intra-particle diffusion in the adsorption process of MB and MO onto the J10-PET thin film. This observation confirms that the adsorption process encompasses multiple sequential steps within the material. When these steps occur independently, the plot typically exhibits intersecting lines, each representing a distinct mechanism—surface adsorption and intra-particle diffusion.[52, 53]

Furthermore, the intercept B_L provides insights into the escalating influence of the boundary layer as the intercept value rises. A higher B_L intercept value signifies a greater abundance of solute adsorption within the boundary layer. The values of B_L, derived from the intercepts of linear qt vs. $t^{1/2}$ plots across all studied conditions, have been compiled in Table 2.

Activation Energy

The Arrhenius equation establishes a relationship between the rate constant and the temperature, which is utilized to estimate the activation energy[47]. Fig. 14 shows the relationship between the rate constant in Table 1 and the corresponding temperature to estimate the activation energy for MB and MO adsorption on a J10-PET thin film.

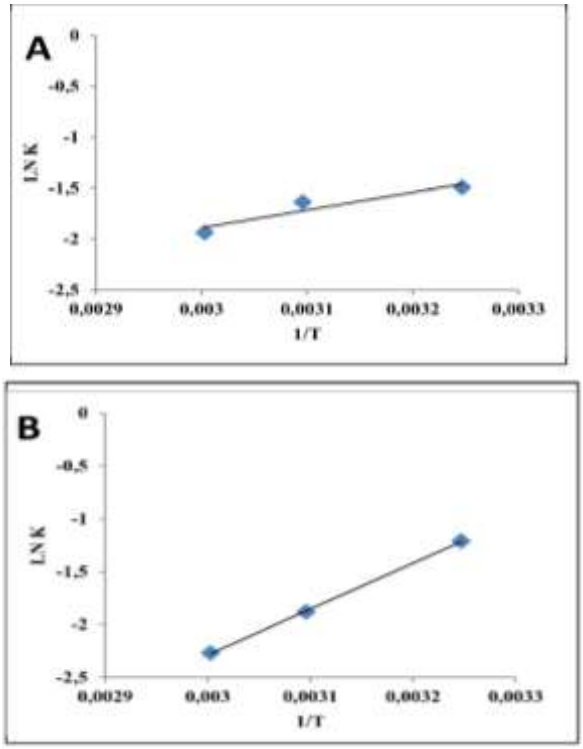

Figure 14. A plot of lnK2 versus 1/T of the adsorption of A) MB B) MO on J10- PET thin film.

The activation energy in adsorption signifies the energy needed to overcome the interactions between the adsorbate (dye molecules) and the adsorbent surface. The value of activation energy for the adsorption of MB and MO onto J10-PET thin film calculated from the slope of the plot is 14.42 and 36.08 kJ/mol for MB and MO, respectively, representing the energy required to initiate the adsorption process for MB and MO onto J10-PET thin film.

Activation energy values provide insights into the energetics and mechanisms of MB and MO adsorption onto the J10-PET thin film. The fact that activation energy values are relatively low suggests that the adsorption process is favorable and relatively easy to initiate, which can be important for designing energy-efficient adsorption processes.

Published Online First: August, 2024
https://doi.org/10.21123/bsj.2024.9373
P-ISSN: 2078-8665 - E-ISSN: 2411-7986
Baghdad Science Journal

Mechanism of Adsorption and Attraction between J10, MB, and MO

The adsorption process is driven by several factors, including surface charge and the presence of compatible functional groups. An examination of the FTIR spectra reveals the mechanisms of attraction between molecule J10 and the dye molecules MB and MO. The adsorption of J10 onto MB and MO is driven by a combination of dipole-dipole interactions, Van der Waals forces, n-π interactions, and, in the case of MB, hydrogen bonding Fig. 15. These complex mechanisms of attraction contribute to the adsorption of J10 onto the dye molecules, providing a comprehensive understanding of the adsorption process.

1- Dipole-Dipole and Van der Waals Interactions:

One of the primary driving forces of attraction involves dipole-dipole interactions and Van der Waals forces:

The carbonyl group (C=O) in J10 plays a central role in these interactions. It has a polar bond, with oxygen being more electronegative, resulting in a partial negative charge on the oxygen atom and a partial positive charge on the carbon atom. MB and MO also contain regions of electron density and electronegative nitrogen and sulfur atoms. These electronegative atoms can interact with the partially positively charged carbon atom or the partially negatively charged oxygen atom in J10, leading to dipole-dipole interactions.

2- Van der Waals forces, specifically London dispersion forces, exist in all molecules due to temporary fluctuations in electron distribution. J10, MB, and MO have nonpolar segments within their structures that can interact through Van der Waals forces. Additionally, the presence of aromatic rings in all three molecules can lead to pi-stacking interactions, where the π-electron clouds of these rings engage in Van der Waals interactions, further enhancing mutual attraction.[54]

3- n-π Interaction:

An additional mechanism contributing to the attraction is the n-π interaction. This arises from the delocalization of the lone pair of electrons on the oxygen atom in J10 into the π orbital of the aromatic rings in the dye molecules. This interaction serves to strengthen the bonding between J10 and MB or MO.[55]

4- Hydrogen Bonding:

In the case of MB and MO, both the nitrogen atom in MB, MO, and the hydrogen atom within the NH group of J10 have the potential to establish hydrogen bonds. This interaction arises from the nitrogen atom in MB and MO functioning as a hydrogen bond acceptor, utilizing its available lone pairs to engage in hydrogen bonding with the hydrogen atom in the NH group of J10.[56]

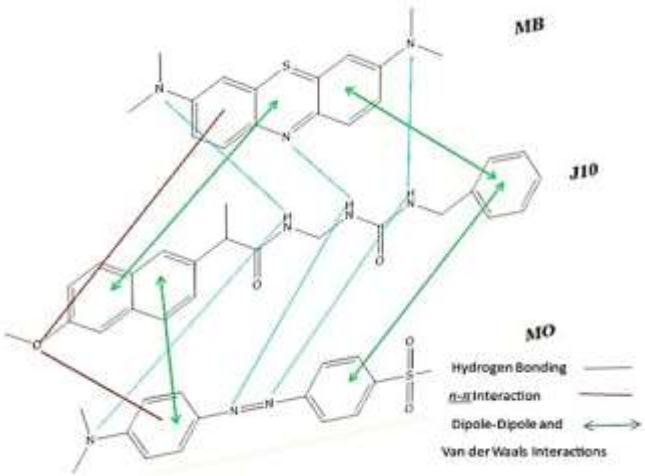

Figure 15. Mechanism of Adsorption and Attraction between J10, MB, and MO

Conclusions

In this study, we introduced an innovative approach utilizing N-(3-benzylureido)(methyl)-2-(6-methoxynaphthalen-2-yl)propanamide (J10) as an additive for recycled PET to create J10-PET thin films. These thin films demonstrated impressive adsorption capabilities, with equilibrium adsorption capacities (Qe) of 19.12 mg/g for MB and 17.065 mg/g for MO. The research emphasized the effectiveness of the J10-PET thin film for the removal of MB and MO from aqueous solutions. The pseudo-second-order model was found to aptly describe the kinetics of adsorption, highlighting the efficiency of the J10-PET thin film. Moreover, the activation energy values of 14.42 kJ/mol for MB and 36.08 kJ/mol for MO underscored the potential of this adsorbent for the effective removal of these pollutants. Our study contributes to a comprehensive understanding of adsorption processes, presenting the J10-PET thin film as a promising and sustainable solution for addressing the removal of MB and MO

Published Online First: August, 2024
https://doi.org/10.21123/bsj.2024.9373
P-ISSN: 2078-8665 - E-ISSN: 2411-7986
Baghdad Science Journal

pollutants in aqueous environments. Future work may focus on further optimization of the J10-PET thin film production, exploration of additional pollutants, and the practical applicability of this adsorbent in real-world environmental scenarios. These results offer promising possibilities for eco-friendly solutions in water purification and pollution control, emphasizing the potential of J10-PET thin films as a sustainable and efficient adsorption technology.

Acknowledgements

The authors extend their sincere gratitude to the University of Duhok's College of Science for providing essential resources, including laboratory facilities, which played a crucial role in enabling the execution of this research project.

Authors' Declaration

- Conflicts of Interest: None.
- We hereby confirm that all the Figures and Tables in the manuscript are ours. Furthermore, any Figures and images, that are not ours, have been included with the necessary permission for re-publication, which is attached to the manuscript.
- Ethical Clearance: The project was approved by the local ethical committee at University of Duhok.
- No animal studies are present in the manuscript.
- No human studies are present in the manuscript.
- No potentially identified images or data are present in the manuscript

Authors' Contributions Statement

J. A., P. H., and H. A. played vital roles in formulating and executing the research, analyzing the outcomes, and drafting the manuscript.

Reference

1. Thamer BM, Aldalbahi A, Moydeen A M, Rahaman M, El-Newehy MH. Modified Electrospun Polymeric Nanofibers and Their Nanocomposites as Nanoadsorbents for Toxic Dye Removal from Contaminated Waters: A Review. Polym. J. 2020; 13(1): 20. https://doi.org/10.3390/polym13010020
2. Chandanshive V, Kadam S, Rane N, Jeon BH, Jadhav J, Govindwar S. In situ textile wastewater treatment in high rate transpiration system furrows planted with aquatic macrophytes and floating phytobeds. Chemosphere. 2020; 252. https://doi.org/10.1016/j.chemosphere.2020.126513
3. El-Kousy SM, El-Shorbagy HG, El-Ghaffar MAA. Chitosan/montmorillonite composites for fast removal of methylene blue from aqueous solutions. Mater Chem Phys. 2020; 254. https://doi.org/10.1016/j.matchemphys.2020.123236
4. Ullah A, Zahoor M, Din WU, et al. Removal of Methylene Blue from Aqueous Solution Using Black Tea Wastes: Used as Efficient Adsorbent. Adsorp Sci Technol. 2022; 2022. https://doi.org/10.1155/2022/5713077
5. Huynh PT, Nguyen DK, Nguyen PH, Dinh VP. Adsorption of Methyl Orange and Methylene Blue from aqueous solutions using thermally treated biomass of pine leaves (Pinus kesiya). Res Sq. 2023: 1: 1-22. https://doi.org/10.21203/rs.3.rs-2862013/v1
6. Yasin SA, Abbas JA, Ali MM, Saeed IA, Ahmed IH. Methylene blue photocatalytic degradation by TiO2 nanoparticles supported on PET nanofibres. In: Mater Today Proc. 2020; 20 (4): 482-487. https://doi.org/10.1016/j.matpr.2019.09.174
7. Ghosh GC, Chakraborty TK, Zaman S, Nahar MN, Kabir AHME. Removal of methyl orange dye from aqueous solution by a low-cost activated carbon prepared from mahagoni (Swietenia mahagoni) Bark. Pollut. 2020; 6(1): 171-184. https://doi.org/10.22059/poll.2019.289061.679
8. Jedynak K, Repelewicz M, Kurdziel K, Wideł D. Mesoporous carbons as adsorbents to removal of methyl orange (Anionic dye) and methylene blue (cationic dye) from aqueous solutions. Desalin Water Trea. 2021; 220: 363-379. https://doi.org/10.5004/dwt.2021.26925
9. Yönten V, Sanyürek NK, Kivanç MR. A thermodynamic and kinetic approach to adsorption of methyl orange from aqueous solution using a low cost activated carbon prepared from Vitis vinifera L. Surf Interfaces. 2020; 20. https://doi.org/10.1016/j.surfin.2020.100529

Published Online First: August, 2024
https://doi.org/10.21123/bsj.2024.9373
P-ISSN: 2078-8665 - E-ISSN: 2411-7986
Baghdad Science Journal

10. Yuan N, Cai H, Liu T, Huang Q, Zhang X. Adsorptive removal of methylene blue from aqueous solution using coal fly ash-derived mesoporous silica material. Adsorp Sci Technol. 2019; 37(3-4): 333-348. http://doi.org/10.1177/0263617419827438
11. Al-Tohamy R, Ali SS, Li F, Okasha K M, G Mahmoud Y, Elsamahy T, et al. A critical review on the treatment of dye-containing wastewater: Ecotoxicological and health concerns of textile dyes and possible remediation approaches for environmental safety. Ecotoxicol Environ Saf. 2022; 231: 113160. https://doi.org/10.1016/j.ecoenv.2021.113160
12. Gao H, Zhao S, Cheng X, Wang X, Zheng L. Removal of anionic azo dyes from aqueous solution using magnetic polymer multi-wall carbon nanotube nanocomposite as adsorbent. Chem Eng J. 2013; 223: 84-90. http://dx.doi.org/10.1016/j.cej.2013.03.004
13. Olisah C, Adams JB, Rubidge G. The state of persistent organic pollutants in South African estuaries: A review of environmental exposure and sources. Ecotoxicol Environ Saf. 2021; 219: 1-18 https://doi.org/10.1016/j.ecoenv.2021.112316
14. Hevira L, Zilfa, Rahmayeni, Ighalo JO, Aziz H, Zein R. Terminalia catappa shell as low-cost biosorbent for the removal of methylene blue from aqueous solutions. J Ind Eng Chem. 2021; 97: 188-199. https://doi.org/10.1016/j.jiec.2021.01.028
15. Soleimani S, Heydari A, Fattahi M, Motamedisade A. Calcium alginate hydrogels reinforced with cellulose nanocrystals for methylene blue adsorption: Synthesis, characterization, and modelling. Ind Crops Prod. 2023; 192: 115999. https://doi.org/10.1016/j.indcrop.2022.115999
16. Hameed BH, Din ATM, Ahmad AL. Adsorption of methylene blue onto bamboo-based activated carbon: Kinetics and equilibrium studies. J Hazard Mater. 2007; 141(3): 819-825. http://doi.org/10.1016/j.jhazmat.2006.07.049
17. Yilmaz E, Guzel Kaya G, Deveci H. Removal of methylene blue dye from aqueous solution by semi-interpenetrating polymer network hybrid hydrogel: Optimization through Taguchi method. J Polym Sci A Polym Chem. 2019; 57(10): 1070-1078.http://doi.org/10.1002/pola.29361
18. Cheah W, Hosseini S, Khan MA, Chuah TG, Choong TSY. Acid modified carbon coated monolith for methyl orange adsorption. Chem Eng J Adv. 2013; 215-216: 747-754.http://dx.doi.org/10.1016/j.cej.2012.07.004
19. Cheng X , Jiang D , Chen H , Barati B , Yuan C , Li H, et al. Multi-stage adsorption of methyl orange on the nitrogen-rich biomass-derived carbon adsorbent: DFT and MD evaluation. Chemosphere. 2023; 338: 139218. http://doi.org/10.1016/j.chemosphere.2023.139218
20. El Gamal M, Mohamed FM, Mekewi MA, Hashem FS, El-Aassar MR, Khalifa RE. Adsorptive removal of methyl orange from aqueous solutions by polyvinylidene fluoride tri-flouro ethylene/carbon nanotube/kaolin nanocomposite: Kinetics, isotherm, and thermodynamics. Desalin Water Treat. 2020; 193: 142-151. http://doi.org/10.5004/dwt.2020.25690
21. Dehghani MH, Salari M, Karri RR, Hamidi F, Bahadori R. Process modeling of municipal solid waste compost ash for reactive red 198 dye adsorption from wastewater using data driven approaches. Sci Rep. 2021; 11(1): 11613. https://doi.org/10.1038/s41598-021-90914-z
22. Zaman S, Biswas P, Zaman R, Islam M S, Mehrab M N, Ghosh G C, et al. Jute (Corchorus olitorius) stick charcoal: a potential bioadsorbent for the removal of Cr(VI) from an aqueous solution .H2Open J. 2022; 5(4): 656-669. http://doi.org/10.2166/h2oj.2022.027
23. Mahmood ZA, Farhan AM, Kadhim NJ, Hade MS. Kinetic and Theoretical Study of Removal Gentian Violet from Aqueous Solution Using Stachy Plant. Baghdad Sci J. 2023; 20 (4):1283. http://doi.org/10.21123/bsj.2023.7066
24. Ahmed FS, AbdulRazak AA, Alsaffar MA. Modelling and optimization of methylene blue adsorption from wastewater utilizing magnetic marble dust adsorbent: A response surface methodology approach. Mater Today Proc. 2022; 60: 1676-1688. http://doi.org/10.1016/j.matpr.2021.12.224
25. Bassim S, Mageed AK, AbdulRazak AA, Majdi HSh. Green Synthesis of Fe3O4 Nanoparticles and Its Applications in Wastewater Treatment. Inorganics.2022; 10(12): 260. http://doi.org/10.3390/inorganics10120260
26. Jayasekara SK, Joni HD, Jayantha B, Jayasekara T, Sivakumar P, Jayakody L, et al. Trends in in-silico guided engineering of efficient polyethylene terephthalate (PET) hydrolyzing enzymes to enable bio-recycling and upcycling of PET. Comput Struct Biotechnol J. 2023; 21: 3513-3521. https://doi.org/10.1016/j.csbj.2023.06.004
27. Rahmawati I, Priyanto A, Darsono T, Sulhadi, Aji MP. The adsorption of dye waste using black carbon from polyethylene terephthalate (PET) plastic bottle waste. J Phys Conf Ser. 2019; 1321(2): 022011. http://doi.org/10.1088/1742-6596/1321/2/022011
28. El Essawy NA, Ali SM, Farag HA, Konsowa AH, Elnouby M, Hamad HA. Green synthesis of graphene from recycled PET bottle wastes for use in the adsorption of dyes in aqueous solution. Ecotoxicol Environ Saf. 2017; 145: 57-68.http://doi.org/10.1016/j.ecoenv.2017.07.014
29. Mallakpour S, Behranvand V. Manufacture and characterization of nanocomposite materials obtained from incorporation of D-glucose functionalized MWCNTs into the recycled poly (ethylene terephthalate). Des Monomers Polym. 2016; 19(4): 283-289. http://dx.doi.org/10.1080/15685551.2015.1136533

Published Online First: August, 2024
https://doi.org/10.21123/bsj.2024.9373
P-ISSN: 2078-8665 - E-ISSN: 2411-7986
Baghdad Science Journal

30. Djahed B, Shahsavani E, Khalili Naji F, Mahvi AH. A novel and inexpensive method for producing activated carbon from waste polyethylene terephthalate bottles and using it to remove methylene blue dye from aqueous solution. Desalin Water Treat. 2016; 57(21): 9871-9880. http://dx.doi.org/10.1080/19443994.2015.1033647
31. Abedsoltan H. A focused review on recycling and hydrolysis techniques of polyethylene terephthalate. Polym Eng Sci. 2023; 63 (9): 2651-2674. http://doi.org/10.1002/pen.26406
32. Chakraborty T K, Audhikary K, Ghosh G C, Rahman M S, Habib A, Islam M S, et al. Adsorption of acid and basic dye from the simulated wastewater using carbonized microplastic particles synthesized from recycled polyethylene terephthalate plastic waste bottles: an integrated approach for experimental and practical applications. Aqua Water Infrastruct. Ecosyst. Soc. 2023; 72(4): 491-506. http://doi.org/10.2166/aqua.2023.211
33. Li S, Cho M K, Yuan X, Deng S , Li H, Zhao L, et al. Cyclic performance evaluation of CO2 adsorption using polyethylene terephthalate plastic-waste-derived activated carbon. Fuel. 2023; 331: 125599. http://doi.org/10.1016/j.fuel.2022.125599
34. Lin T H, Phat L N, Tu P M, Thang T Q, Khoa B D D, Lam C V, et al. Recycled Polyethylene Terephthalate Fibers Aerogels Modified with Graphene Oxide for Adsorption of Methylene Blue and Coated with Polydimethylsiloxane Tetraethyl Orthosilicate for Oil Removal. J Polym Environ. 2023; 31(2): 648-663. http://doi.org/10.1007/s10924-022-02607-x
35. Taşçı Y, Kaptanoğlu İG, Sert Ş. Using PET (polyethylene terephthalate) wastes as an adsorbent for Ce(III) and Sr(II) removal from aqueous solution. J Radioanal Nucl Chem. 2023; 332: 4767–4779. http://doi.org/10.1007/s10967-023-08889-2
36. Soltanolzakerin-Sorkhabi T, Fallahi-Samberan M, Kumaravel V. Antimicrobial Activities of Polyethylene Terephthalate-Waste-Derived Nanofibrous Membranes Decorated with Green Synthesized Ag Nanoparticles. Molecules. 2023; 28(14): 5439.http://doi.org/10.3390/molecules28145439
37. Oliveira ZM, Teixeira S, Souza E, Souza C, Pessoa R. Reverse Logistics: an approach to raising awareness of the risks caused by the incorrect disposal of expired drugs. DJFM. 2023; 6(1): 21813. http://doi.org/10.55267/djfm/13423
38. Ojeda L, Oliva J, Oliva AI, Garcia CR. Recycling expired pharmaceutical drugs as redox materials for efficient and sustainable flexible supercapacitors. New J Chem. 2023; 47(21): 10090-10104. http://doi.org/10.1039/D3NJ00497J
39. Freitas L de AA, Radis-Baptista G. Pharmaceutical Pollution and Disposal of Expired, Unused, and Unwanted Medicines in the Brazilian Context. J Xenobiot. 2021; 11(2): 61-76.http://doi.org/10.3390/jox11020005
40. Diriba G, Hasen G, Tefera Y, Suleman S. Assessment of the magnitude and contributing factors of expired medicines
in the public pharmaceutical supply chains of Wester n Ethiopia. BMC Health Serv Res. 2023; 23(1): 791. http://doi.org/10.1186/s12913-023-09776-y
41. Mgharbel M, Halawy L, Milane A, Zeaiter J, Saad W. Pyrolysis of pharmaceuticals as a novel means of disposal and material recovery from waste for a circular economy. J Anal Appl Pyrolysis. 2023; 172: 106014. http://doi.org/10.1016/j.jaap.2023.106014
42. Yasin SA, Abbas JA, Saeed IA, Ahmed IH. The application of green synthesis of metal oxide nanoparticles embedded in polyethylene terephthalate nanofibers in the study of the photocatalytic degradation of methylene blue. Polym Bull. 2020; 77(7): 3473-3484.http://doi.org/10.1007/s00289-019-02919-4
43. Azhar SMA, Samsudin AS, Ismail WNW, Samah NA. Kinetic Modeling Characterization of Cellulose Modified Surface for Methylene Blue Removal from Aqueous Media. Macromol Symp. 2021; 397(1). http://doi.org/10.1002/masy.202000239
44. Abdullah AH, Yasin SA, Abdullah SM, Khalaf MY, Saeed IA. A kinetic and isotherm study on removing methylene blue from aqueous solutions by oxidized cellulose nanostructure. Emergent Mater. 2022; 5(4): 1199-1212. http://doi.org/10.1007/s42247-022-00397-5
45. Ji Y, Yang X, Ji Z, Zhu L, Ma N, Chen D, et al. DFT-Calculated IR Spectrum Amide I, II, and III Band Contributions of N -Methylacetamide Fine Components. ACS Omega. 2020; 5(15): 8572-8578. http://doi.org/10.1021/acsomega.9b04421
46. Subhash, Chaudhary A, Mamta Jyoti. Synthesis, structural characterization, thermal analysis, DFT, biocidal evaluation and molecular docking studies of amide-based Co(II) complexes. Chem Pap. 2023; 77: 5059–5078 http://doi.org/10.1007/s11696-023-02843-y
47. Acemioğlu B. Batch kinetic study of sorption of methylene blue by perlite. Chem Eng J Adv. 2005; 106(1): 73-81. http://doi.org/10.1016/j.cej.2004.10.005
48. Mohammed FF. Equilibrium, Kinetic, and Thermodynamic Study of Removing Methyl Orange Dye from Aqueous Solution Using Zizphus spina-christi Leaf Powder. Baghdad Sci J. 2023; 20(2): 0296. http://doi.org/10.21123/bsj.2022.7036
49. Tran T H, Le A H, Pham T H, Nguyen D T, Chang S W, Chung W J, et al. Adsorption isotherms and kinetic modeling of methylene blue dye onto a carbonaceous hydrochar adsorbent derived from coffee husk waste. Sci Total Environ. 2020; 725: 138325. http://doi.org/10.1016/j.scitotenv.2020.138325

Published Online First: August, 2024
https://doi.org/10.21123/bsj.2024.9373
P-ISSN: 2078-8665 - E-ISSN: 2411-7986
Baghdad Science Journal

50. Ibupoto A S, Qureshi U A, Ahmed F, Khatri Z, Khatri M, Maqsood M, et al. Reusable carbon nanofibers for efficient removal of methylene blue from aqueous solution. Chem Eng Res Des. 2018; 136: 744-752. http://doi.org/10.1016/j.cherd.2018.06.035
51. Ahmed HA, Saleem PH, Yasin SA, Saeed IA. A kinetic study of removing methylene blue from aqueous solutions by modified electrospun polyethelene terephthalate nanofibres. Egypt J Chem. 2021; 64(6): 2803-2813. http://doi.org/10.21608/ejchem.2021.54843.3146
52. de Franco MAE, de Carvalho CB, Bonetto MM, Soares R de P, Féris LA. Removal of amoxicillin from water by adsorption onto activated carbon in batch process and fixed bed column: Kinetics, isotherms, experimental design and breakthrough curves modelling. J Clean Prod. 2017; 161: 947-956. http://doi.org/10.1016/j.jclepro.2017.05.197
53. Abdel-Khalek AA, Abdel-Hafeez MM, Mohamed RA, Gabrail EH. Insights into removal of Eriochrome Black-T dye from aqueous solution by Doum fruit as a natural adsorbent. Egypt J Chem. 2022; 65(7): 189-199. http://doi.org/10.21608/ejchem.2021.100948.4692
54. Thakuria R, Nath NK, Saha BK. The Nature and Applications of π–π Interactions: A Perspective. Cryst Growth Des. 2019; 19(2): 523-528. http://doi.org/10.1021/acs.cgd.8b01630
55. Jawad AH, Abdulhameed AS. Mesoporous Iraqi red kaolin clay as an efficient adsorbent for methylene blue dye: Adsorption kinetic, isotherm and mechanism study. Surf Interfaces. 2020; 18: 100422. http://doi.org/10.1016/j.surfin.2019.100422
56. Ahmad T, Danish M, Rafatullah M, Ghazali A, Sulaiman O, Hashim R, et al. The use of date palm as a potential adsorbent for wastewater treatment: a review. Environ Sci Pollut Res Int. 2012; 19(5): 1464-1484. http://doi.org/10.1007/s11356-011-0709-8.

الابتكار الأخضر في المعالجة البيئية: الأغشية الرقيقة J10-PET لإزالة ملوثات الميثيلين الأزرق والميثيل البرتقالي بكفاءة

جيهان أحمد مصطفى[1] ,بروين هاشم سليم[1] ,هدى أحمد بشير[2]

[1]قسم الكيمياء، كلية العلوم، جامعة دهوك، دهوك، العراق.
[2]قسم الكيمياء، كلية العلوم، جامعة زاخو، دهوك، العراق.

الخلاصة

تتناول هذه الدراسة التحديات البيئية الحرجة المتعلقة بمعالجة مياه الصرف، وتصريف الأدوية المنتهية الصلاحية، والتخلص من النفايات الصلبة مثل البولي إيثيلين تيريفثالات PET. يركز البحث على نهج مبتكر باستخدام N-(3-benzylureido)(methyl)-2-(6-methoxynaphthalen-2-yl)propanamide (J10) كمادة مضافة لبولي إيثيلين تيريفثالات (PET) المعاد تدويره من زجاجات المياه المستهلكة، وإنشاء فيلم رقيق سهل التحضير(J10-PET). تشمل الدراسة تحليلًا مقارنًا بين الأفلام الرقيقة المصنعة من PET النقية والأفلام الرقيقه المصنعة من PET المعدلة بواسطة J10، باستخدام تقنيات متقدمة مثل FTIR وSEM للحصول على رؤى حول الخصائص الهيكلية والمورفولوجية لها. وللإشارة، تظهر الأفلام الرقيقة المطورة فعالية ملحوظة في استخراج الأزرق الميثيلين (MB) والبرتقالي الميثيلين (MO) من الحلول المائية. تركز الدراسة بشكل أساسي على كشف النقاب عن السلوكيات الحركية والتوازن التي تحكم إزالة الميثيلين الأزرق (MB) والبرتقالي الميثيلين (MO). تتضمن الدراسة تحديد سعات الامتصاص في التوازن (qe) للميثيلين الأزرق (MB) والبرتقالي الميثيلين (MO) عند درجات حرارة مختلفة (35، 50، و60 درجة مئوية) وتراكيز مختلفة (5، 10، و15 ملغم/جم). وبشكل ملحوظ، يتبين أن النموذج الزائف من الدرجة الثانيه هو الأنسب لشرح السيناريو الحركي لكل من الميثيلين الأزرق (MB) والبرتقالي الميثيلين (MO). وعلاوة على ذلك، وجد ان الطاقة النشطة (Ea) المرتبطة بامتصاص الميثيلين الأزرق (MB) والبرتقالي الميثيلين (MO) على الفيلم الرقيق J10-PET بقيمة 14.42 كيلوجول/مول و36.08 كيلوجول/مول على التوالي. تسهم هذه النتائج بشكل جماعي في فهم شامل لعملية الامتصاص، مما يلقي الضوء على إمكانية استخدام فيلم PET الرقيق J10 كحلا فعالا لمعالجة إزالة الملوثات الزرقاء الميثيلين (MB) والبرتقالية الميثيلين (MO) من البيئات المائية

الكلمات المفتاحية: الأمتزاز، الأدوية منتهية الصلاحية، الحركية، صبغة المثيلين الأزرق، صبغة المثيل البرتقالي، النفايات الصلبة من البولي أثلين تيرفثاليت، الأغشية الرقيقة، معالجة مياه الصرف الصحي.